Characterization of AMN107, a selective inhibitor of native and mutant Bcr-Abl

Ellen Weisberg,[1,5] Paul W. Manley,[2,5] Werner Breitenstein,[2] Josef Brüggen,[2] Sandra W. Cowan-Jacob,[2] Arghya Ray,[1] Brian Huntly,[3] Doriano Fabbro,[2] Gabriele Fendrich,[2] Elizabeth Hall-Meyers,[1] Andrew L. Kung,[1,4] Jürgen Mestan,[2] George Q. Daley,[4] Linda Callahan,[1] Laurie Catley,[1] Cara Cavazza,[1] Azam Mohammed,[4] Donna Neuberg,[1] Renee D. Wright,[3] D. Gary Gilliland,[3] and James D. Griffin[1,*]

[1]Dana-Farber Cancer Institute, Boston, Massachusetts 02115
[2]Novartis Institutes for Biomedical Research, Basel, CH-4002, Switzerland
[3]Brigham and Women's Hospital, Boston, Massachusetts 02115
[4]Children's Hospital, Boston, Massachusetts 02115
[5]These authors contributed equally to this work.
*Correspondence: james_griffin@dfci.harvard.edu

Summary

The Bcr-Abl tyrosine kinase oncogene causes chronic myelogenous leukemia (CML) and Philadelphia chromosome-positive (Ph+) acute lymphoblastic leukemia (ALL). We describe a novel selective inhibitor of Bcr-Abl, AMN107 (IC_{50} < 30 nM), which is significantly more potent than imatinib, and active against a number of imatinib-resistant Bcr-Abl mutants. Crystallographic analysis of Abl-AMN107 complexes provides a structural explanation for the differential activity of AMN107 and imatinib against imatinib-resistant Bcr-Abl. Consistent with its in vitro and pharmacokinetic profile, AMN107 prolonged survival of mice injected with Bcr-Abl-transformed hematopoietic cell lines or primary marrow cells, and prolonged survival in imatinib-resistant CML mouse models. AMN107 is a promising new inhibitor for the therapy of CML and Ph+ ALL.

Introduction

Chronic myelogenous leukemia (CML) constitutes about 15% of adult leukemias and annually affects 1–2 people per 100,000. The disease progresses in three phases (O'Dwyer et al., 2002): the initial chronic phase, which has a median duration of 4–6 years, is a clonal myeloproliferative disorder characterized by a massive accumulation of functional granulocytes and immature myeloid cells in blood, marrow, and spleen. In untreated patients, the disease may progress via an accelerated phase, characterized by the appearance of undifferentiated blast cells in blood and bone marrow, to a terminal blast crisis phase of the disease. In the blastic phase, for which median survival is 18 weeks, more than 30% of the blood and bone marrow cells are blasts, and myeloid precursors may also form tumors in the lymph nodes, skin, and bone (Kantarjian and Talpaz, 1988).

The underlying cause of CML is the *BCR-ABL* oncogene, which results from a reciprocal t(9;22) chromosome translocation in a hematopoietic stem cell (Deininger et al., 2000). This fusion gene encodes a chimeric Bcr-Abl protein, in which the tyrosine kinase activity of Abl is constitutively activated. CML patients express the 210 kDa Bcr-Abl, whereas patients with Ph+ ALL usually express a p190 kDa Bcr-Abl protein arising from a different breakpoint in the *BCR* gene (Melo et al., 1994; Ravandi et al., 1999).

Expression of either p210 or p190 Bcr-Abl in hematopoietic cell lines abrogates the growth factor requirements for cell proliferation and survival by three major mechanisms: constitutive activation and enhancement of mitogenic signaling (Puil et al., 1994), reduced responsiveness to apoptotic stimuli (Bedi et al., 1994), and altered adhesion to stroma cells and extracellular matrix (Gordon et al., 1987). The constitutively activated tyrosine kinase of Bcr-Abl is essential for the transforming activity (Lugo et al., 1990).

Imatinib mesylate (Gleevec, STI571; Novartis Pharma AG) is a drug targeting the tyrosine kinase activity of Bcr-Abl (Buchdunger et al., 2001) and is an effective therapy for CML. After a median 19 months of treatment, newly diagnosed patients show an estimated 97% complete hematological response (CHR) and 76% complete cytogenetic response (CCR; no detectable Ph+ cells) (O'Brien et al., 2003). However, in ALL or in CML patients who have progressed to either the accelerated or blastic phases of the disease, response rates to imatinib

SIGNIFICANCE

Imatinib is an effective therapy for chronic phase CML, but advanced stage CML and Ph+ ALL patients frequently relapse due to the development of resistance caused by point mutations within the kinase domain of Bcr-Abl. New Abl kinase inhibitors with higher potency against native and imatinib-resistant mutants of Bcr-Abl could have substantial clinical utility. AMN107 is a high-affinity inhibitor that targets many imatinib-resistant mutants of Bcr-Abl, and which may therefore be useful in CML, reducing the incidence of resistant mutants, and in the treatment of imatinib-resistant disease.

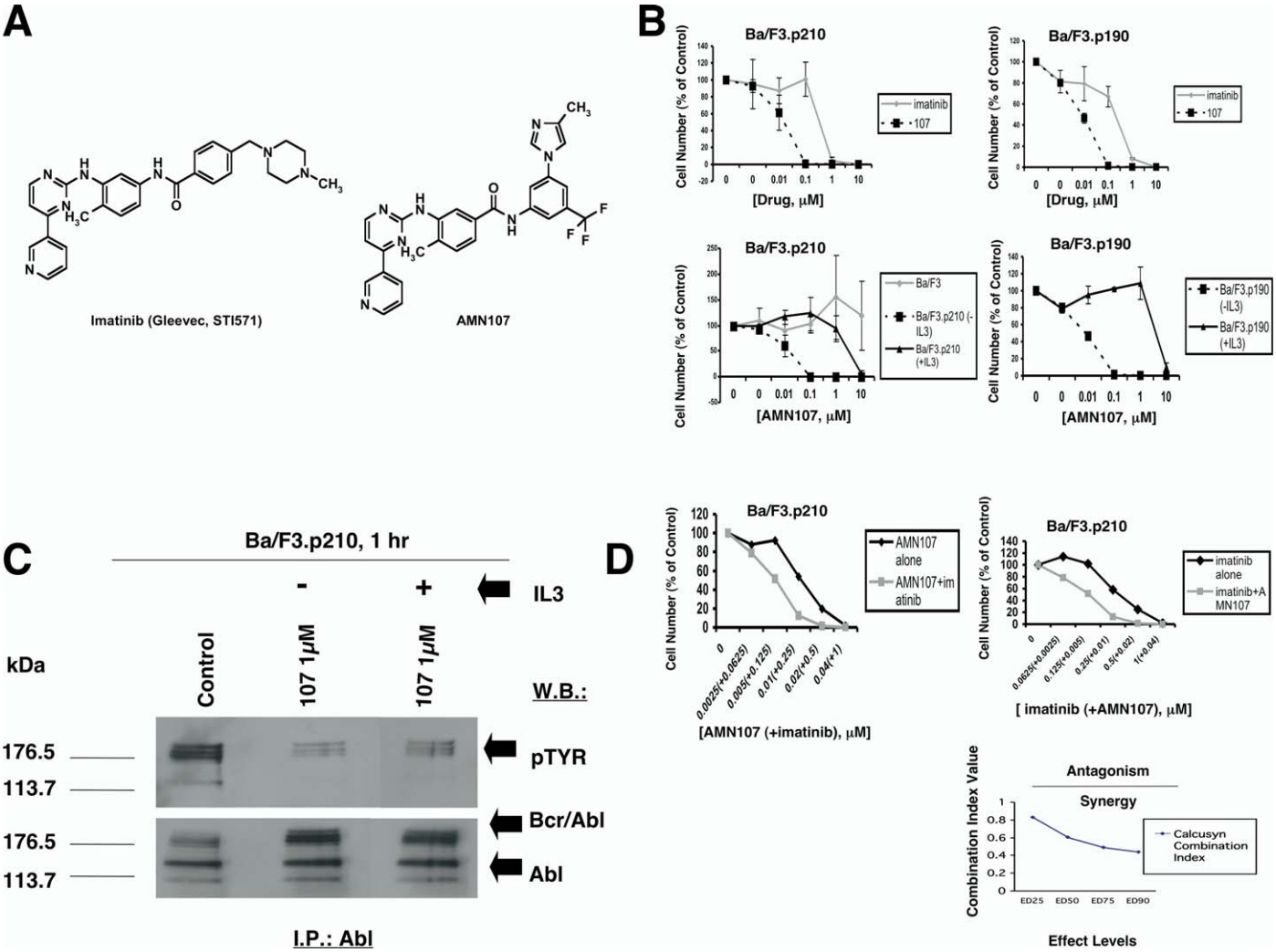

Figure 1. Effects of AMN107 on Bcr-Abl-expressing cell lines in vitro

A: The chemical structures of imatinib and AMN107.

B: Comparison of effects of 3-day treatment of Bcr-Abl-expressing cell lines with imatinib and AMN107 (upper panels), in the presence and the absence of WEHI conditioned medium as a source of IL-3 (lower panels). Bars are SEM, n = 2. In all dose-response curves, viable cell counts are represented as percent of control cells for each drug dose, and were determined by trypan blue exclusion assay.

C: Inhibition of Bcr-Abl autophosphorylation by AMN107 in Bcr-Abl-expressing cells. Autophosphorylation was determined by Bcr-Abl immunoprecipitation, followed by a pTyr immunoblot. Treatment with AMN107 was carried out in both the absence and the presence of IL-3.

D: Dose-response curves generated for combinations of AMN107 and imatinib against Ba/F3.p210 (upper panels), demonstrating synergy (lower panel). Combination studies using Ba/F3.p210 were performed in duplicate; shown are the data for one representative experiment.

therapy are significantly decreased and, of those who initially respond to treatment, many relapse within 12 months. Relapse is often associated with point mutations in Bcr-Abl that reduce the binding affinity of imatinib, or occasionally with amplification of the *BCR-ABL* gene (Gorre et al., 2001; Cowan-Jacob et al., 2004; le Coutre et al., 2000; Weisberg and Griffin, 2000; Mahon et al., 2000; Campbell et al., 2002; Hochhaus et al., 2002; Morel et al., 2003). Thus, there is a need for additional Bcr-Abl tyrosine kinase inhibitors that are more potent and active against imatinib-resistant Bcr-Abl mutants.

The molecular details of the interaction of imatinib with the Abl kinase domain have been revealed from crystal structures of complexes (Schindler et al., 2000; Nagar et al., 2003; Cowan-Jacob et al., 2004), and further supported by an analysis of the effects on binding of point mutations in the protein (Cowan-Jacob et al., 2004). Based upon this structural data, we hypothesized that more potent and selective compounds could be designed by incorporating alternative binding groups for the *N*-methylpiperazine group, while retaining an amide pharmacophore to maintain the H-bond interactions to Glu286 and Asp381 (Manley et al., 2004). This approach resulted in the discovery of AMN107 (Figure 1A), and here we detail the characterization of this molecule in vitro and in experimental Bcr-Abl-driven models of leukemia in mice. AMN107 has superior potency to imatinib as an inhibitor of Bcr-Abl in vitro and in vivo. Furthermore, we report on the efficacy of AMN107 in inhibiting some imatinib-resistant mutant forms of the kinase both in vitro and in vivo.

Table 1. Comparison of imatinib and AMN107 for effects on autophosphorylation and proliferation in cells

	Imatinib (IC_{50} in nM)		AMN107 (IC_{50} in nM)	
Kinase (cell type)	Autophosphorylation	Proliferation	Autophosphorylation	Proliferation
wt-32D + IL-3	NA	6140 ± 449, n = 14	NA	6134 ± 228, n = 3
wt-Ba/F3 + IL-3	NA	7384 ± 766, n = 5	NA	>10000, n = 15
p210 Bcr-Abl (32D)	194 ± 7, n = 94	334 ± 37, n = 23	20 ± 1, n = 53	9.2 ± 0.3, n = 3
Bcr-Abl (K562)	470 ± 59, n = 15	272 ± 27, n = 21	43 ± 15, n = 3	12 ± 2, n = 3
Bcr-Abl (Ku-812F)	466 ± 59, n = 7	80 ± 35, n = 13	60 ± 19, n = 5	8 ± 2, n = 6
p210 Bcr-Abl (Ba/F3)	220 ± 36, n = 12	649 ± 52, n = 18	21 ± 2, n = 5	25 ± 2, n = 49
p190 Bcr-Abl (Ba/F3)	122 ± 15, n = 3		33 ± 4, n = 3	
E255K Bcr-Abl (Ba/F3)	2108 ± 367, n = 3	>6000, n = 3	150 ± 12, n = 3	566 ± 107, n = 3
E255V Bcr-Abl (Ba/F3)	6499 ± 666, n = 13	6368 ± 892, n = 11	246 ± 36, n = 8	681 ± 72, n = 12
T315I Bcr-Abl (Ba/F3)	>10000, n = 20	7393 ± 157, n = 3	>10000, n = 12	>10000, n = 15
F317L Bcr-Abl (Ba/F3)	818 ± 99, n = 10	1583 ± 236, n = 14	41 ± 5, n = 8	80 ± 6, n = 11
M351T Bcr-Abl (Ba/F3)	595 ± 63, n = 10	1285 ± 180, n = 13	31 ± 4, n = 8	33 ± 3, n = 10
F486S Bcr-Abl (Ba/F3)	1230 ± 121, n = 10	2728 ± 676, n = 7	43 ± 6, n = 4	87 ± 4, n = 4
M244V Bcr-Abl (Ba/F3)	NA	3100^{*wst}, n = 1	NA	39^{wst}, n = 1
L248R Bcr-Abl (Ba/F3)	NA	$>20000^{*wst}$, n = 1	NA	919^{wst}, n = 1
Q252H Bcr-Abl (Ba/F3)	NA	2900^{*wst} , n = 1	NA	16^{wst}, n = 1
Y253H Bcr-Abl (Ba/F3)	NA	17700^{*wst} , n = 1	NA	751^{wst}, n = 1
E279K Bcr-Abl (Ba/F3)	NA	9900^{*wst} , n = 1	NA	75^{wst}, n = 1
E282D Bcr-Abl (Ba/F3)	NA	1300^{*wst} , n = 1	NA	39^{wst}, n = 1
V289S Bcr-Abl (Ba/F3)	NA	1400^{*wst} , n = 1	NA	7^{wst}, n = 1
L384M Bcr-Abl (Ba/F3)	NA	2800^{*wst} , n = 1	NA	39^{wst}, n = 1
G250E Bcr-Abl (Ba/F3)	NA	4800^{*wst} , n = 1	NA	219^{wst}, n = 1
PDGFR-α + PDGFR-β (A31)	74 ± 11, n = 11		71 ± 7, n = 20	
PDGFR-β (Tel Ba/F3	NA	39 ± 4, n = 8	NA	57 ± 7, n = 18
c-Kit exon13 mutant (GIST882)	96 ± 12, n = 7	120 ± 6, n = 15	200 ± 13, n = 19	160 ± 12, n = 17
c-Kit del 560-561 (Ba/F3)	27, n = 1	27 ± 2, n = 2	27 ± 3, n = 3	26 ± 1, n = 4
VEGFR-2 (CHO-VEGFR2)	>10000, n = 6		3720 ± 920, n = 5	NA
c-erbB-2 (BT-474)	>10000, n = 4		>10000, n = 2	>10000, n = 6
c-erbB-2 (Ba/F3-erbB-2)		$>3000^{AB}$, n = 2		$>3000^{AB}$, n = 2
Flt3-ITD (Ba/F3-NPOS)		$>3000^{AB}$, n = 2		$>3000^{AB}$, n = 2
Ret (Ba/F3-PTC-3)		$>3000^{AB}$, n = 2		$>3000^{AB}$, n = 2
Met (Ba/F3-Tpr-Met)		$>3000^{AB}$, n = 2		$>3000^{AB}$, n = 2
IGF-1R (NWT-21)	>10000, n = 1		>10000, n = 4	
Ins-R (A14)	>10000, n = 1		>10000, n = 4	
FGFR-1 (Ba/F3-Bcr-FGFR1)		$>3000^{AB}$, n = 3		$>3000^{AB}$, n = 2
JAK-2 (Ba/F3-JAK-2)		$>3000^{AB}$, n = 2		$>3000^{AB}$, n = 2
Ras (Ba/F3-H-Ras-G12V)		$>3000^{AB}$, n = 2		$>3000^{AB}$, n = 2
NPM-Alk (Ba/F3-NPM-Alk cl. 1)		$>3000^{AB}$, n = 2		$>3000^{AB}$, n = 2
Akt (Ba/F3-MyrAkt, cl. 21)		>3000, n = 1		>3000, n = 2

The influence of compounds on kinase autophosphorylation or cell viability was calculated as percentage inhibition. Dose-response curves were used to calculate IC_{50} values, expressed as mean ± SEM, n = number of experiments. The antiproliferative activity was assessed using either the ATPlite assay kit (Perkin-Elmer) or, where indicated (^{AB}), the Alamar Blue assay kit (Biosource International Inc.). ^{wst}, WST-1 reagent (Roche), as previously described (Azam et al., 2003), was used to generate IC50 values. *, values as reported previously for imatinib (Azam et al., 2003)

Results

AMN107 selectively inhibits proliferation of Bcr-Abl-expressing cells and inhibits Bcr-Abl autophosphorylation

AMN107 inhibited the proliferation of Ba/F3 cells expressing p210- and p190-Bcr-Abl, or K562 and Ku-812F cells with IC_{50} values $\leq$12 nM (Figure 1B and Table 1). AMN107 was at least 10-fold more potent than imatinib against Bcr-Abl expressing cell lines, but like imatinib, did not inhibit untransformed Ba/F3 cells growing in IL-3 at concentrations $\leq$6 μM. Ba/F3 cells expressing p210 and p190 Bcr-Abl could also be partially rescued from the inhibitory effects of up to 1 μM AMN107 when cultured in the presence of IL-3 (Figure 1B). At concentrations of AMN107 higher than 1 μM, cells died even in the presence of IL-3 (Figure 1B and Supplemental Data). Inhibition of cell growth by AMN107 was associated with induction of apoptosis (Supplemental Data). AMN107 did not reduce the formation of normal human myeloid and erythroid progenitor cells (assayed as CFU-GM [colony-forming unit, granulocyte/macrophage] and BFU-E [burst-forming unit, erythroid]) at concentrations $\leq$100 nM, but resulted in ~50% reduction in colony numbers at 1 μM (Supplemental Data). In preliminary mouse tolerability studies, AMN107 (50 or 150 mg/kg p.o. b.i.d. for 14 days) was well tolerated, and there were no significant reductions in blood erythrocytes, reticulocytes, leukocytes, or platelets.

AMN107 potently inhibited proliferation of cells transformed by activated mutants of Arg, Kit, PDGFRα, and PDGFRβ (Table 1 and Supplemental Data), but had no significant effect on the viability or proliferation of Ba/F3 cells rendered factor-independent through expression of activated forms of erbB2, Flt3, Met, Ret, IGF-1R, or NPM-ALK, and several other tyrosine kinases at concentrations $\leq$3 μM (Table 1). Taken together, these data suggest that AMN107 selectively inhibits Bcr-Abl, Kit, and PDGFR tyrosine kinases, but does not significantly affect any of the kinases required for IL-3 signaling, such as JAK2, or a

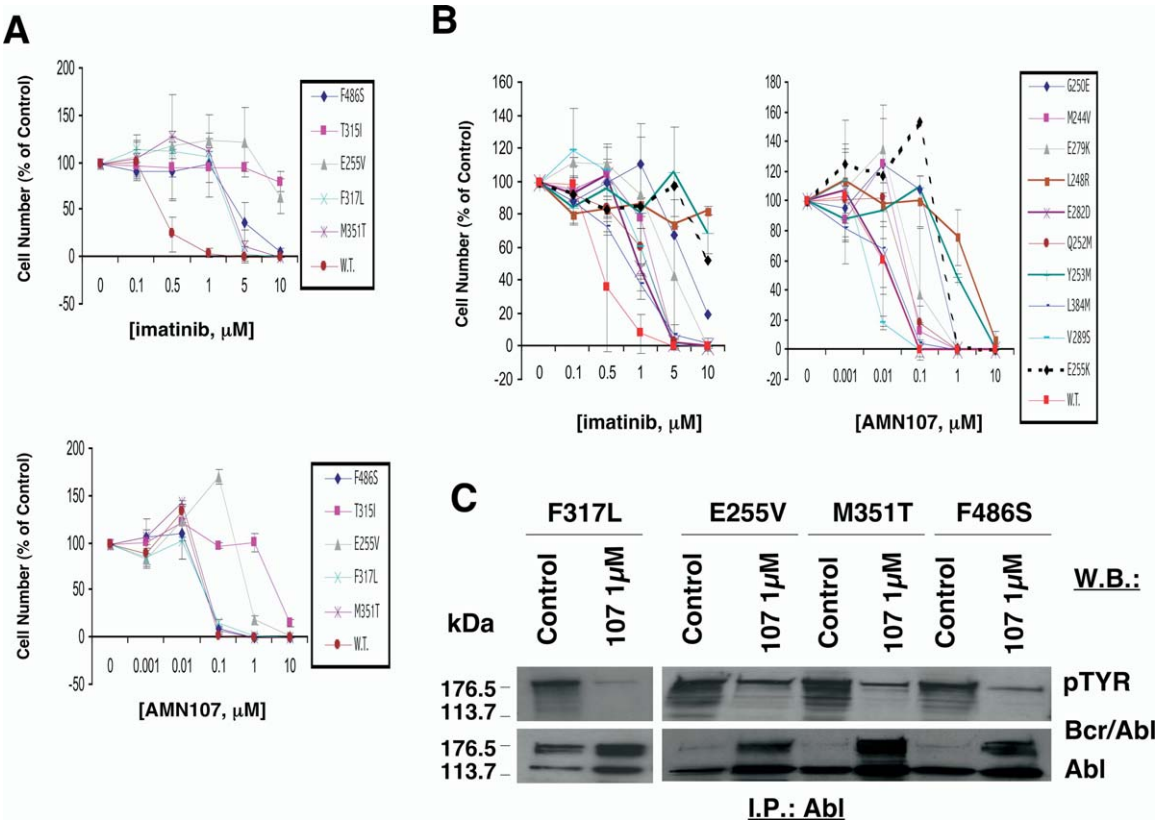

Figure 2. Effects of AMN107 on imatinib-resistant and wild-type Bcr-Abl-expressing cells in vitro

A and B: Treatment of Bcr-Abl mutant-expressing and wild-type Bcr-Abl-expressing Ba/F3 cells with imatinib versus AMN107. **A:** Upper panel: Imatinib treatment; bars are SEM, n = 3. Lower panel: AMN107 treatment, n = 3. **B:** Left panel: Imatinib treatment. Right panel: AMN107 treatment, n = 2.
C: Inhibition of Bcr-Abl autophosphorylation by AMN107 in imatinib-resistant Bcr-Abl-expressing cells. Bcr-Abl autophosphorylation was determined as in Figure 1C.

broad variety of other receptor tyrosine kinases or tyrosine kinase oncogenes. Furthermore, in cell-free assays, AMN107 at concentrations <3 μM had no significant effect on transphosphorylation catalyzed by the GST-fusion kinase domains of CDK-1, FGFR-1, Flt-3, HER-1, IGF-1R, InsR, c-Met, PKA, PKB, c-Src, Tie-2, or VEGFR-2 (data not shown).

Imatinib and AMN107 were compared quantitatively via capture ELISA for their effects on cellular Bcr-Abl autophosphorylation activity and on Bcr-Abl-dependent cell proliferation (Table 1). AMN107 (IC_{50} 20–60 nM) was consistently more potent than imatinib (IC_{50} 120–470 nM) in inhibiting Bcr-Abl tyrosine kinase activity in cell lines. In the presence of IL-3, AMN107 inhibited autophosphorylation but no longer inhibited cell viability (Figures 1B and 1C).

Exposure of Ba/F3.p210 (Figure 1D) or Ba/F3.p190 (data not shown) cells to both AMN107 and imatinib simultaneously across a range of concentrations resulted in synergistic cytotoxicity.

AMN107 selectively inhibits the proliferation of imatinib-resistant Bcr-Abl-expressing cells and autophosphorylation of imatinib-resistant Bcr-Abl mutants

Imatinib and AMN107 were compared for effects on cells expressing point mutants of Bcr-Abl associated with imatinib resistance in patients (Hofmann et al., 2002; Shah et al., 2002; von Bubnoff et al., 2002; Branford et al., 2002; Roche-Lestienne et al., 2002). A series of Ba/F3 cell lines stably expressing E255V, T315I, F317L, M351T, F486S, G250E, M244V, L248R, Q252H, Y253H, E255K, E279K, E282D, V289S, and L384M Bcr-Abl mutants were generated after transfection with expression plasmids containing each mutant (Azam et al., 2003).

As reported, imatinib effectively inhibited proliferation of Ba/F3 cells expressing nonmutated Bcr-Abl, but was substantially less active against cells expressing any of these Bcr-Abl point mutants (IC_{50} values $\geq$1 μM; Figure 2A, 2B, and Table 1) (Cowan-Jacob et al., 2004). In contrast, AMN107 inhibited proliferation of Ba/F3 cells expressing G250E, E255K(V), F317L, M351T, F486S, M244V, L248R, Q252H, Y253H, E255K, E279K, E282D, V289S, and L348M Bcr-Abl mutants at <1 μM concentrations (Table 1). However, the T315I mutant remained resistant to AMN107 below 10 μM. Also, four of these mutants had IC_{50} values >500 nM (E255K[V], L248R, Y253H), indicating intermediate sensitivity. AMN107-induced cytotoxicity of Ba/F3 cells expressing E255V, F317L, M351T, and F486S mutants could be rescued by the addition of IL-3, suggesting that the critical target was probably Bcr-Abl itself (Supplemental Data).

Similarly, AMN107, in contrast to imatinib, potently inhibited the tyrosine autophosphorylation of the E255K, E255V, F317L, M351T, and F486S Bcr-Abl mutants with mean IC_{50} values of

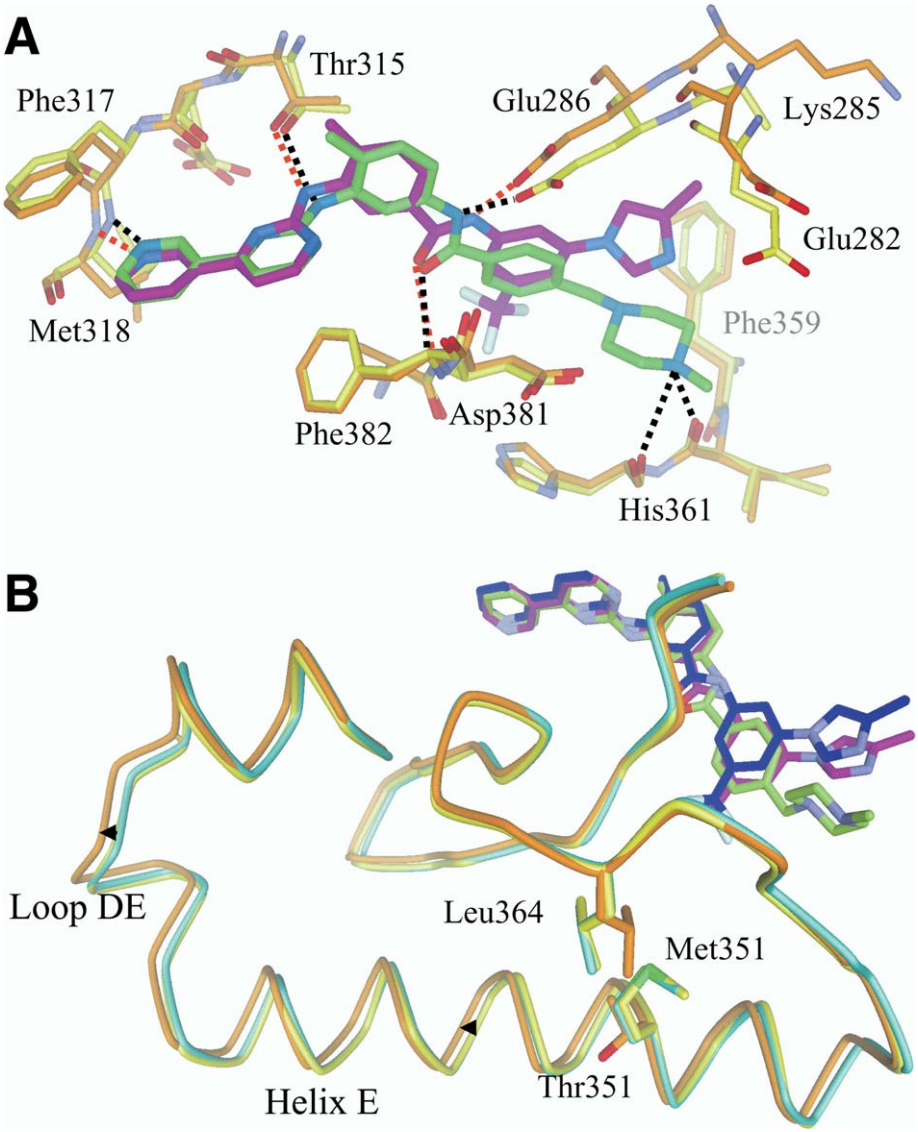

Figure 3. Abl-AMN107 complex

A: Superposition of AMN107 (magenta) bound to Abl^{M351T} (orange), and imatinib (green) bound to Abl (yellow). H bonds within the AMN107-Abl^{M351T} complex are depicted as dashed red lines, whereas those in the imatinib complex are shown in black. The variability in the positions of side chains from the C-helix (top right corner) is due to crystal contacts that influence the position of the N-terminal lobe of the kinase. The methyl-imidazole group of AMN107 packs in a hydrophobic pocket formed by these residues with the nitrogen exposed to solvent.

B: Superposition of parts of the backbone structures of imatinib-Abl (yellow), AMN107-Abl^{M351T} (orange), and AMN107-Abl (cyan). The inhibitors are shown in green, magenta and blue, respectively. The small black arrows show the shifts within helix E and the preceding loop, DE.

150, 246, 41, 31, and 43 nM, respectively (Figure 2C and Table 1). These effects were not associated with a decrease in Abl or Bcr-Abl protein levels (Figure 2C and Supplemental Data). Autophosphorylation of the T315I mutant was unaffected by AMN107. Overall, these results indicate that many imatinib-resistant Bcr-Abl mutants are relatively or absolutely more sensitive to AMN107.

AMN107 also inhibited ligand-induced cellular PDGFR kinase activity and the growth of cells whose proliferation is dependent on activated forms of PDGFR with mean IC_{50} values of 71 and 57 nM (Table 1). In addition, AMN107 inhibited constitutively activated (autophosphorylated) c-Kit, harboring gain-of-function mutations in exon-13 (GIST882 cells) or exon-11 (juxtamembrane domain deletion 560–561, expressed in Ba/F3 cells), with mean IC_{50} values of 200 nM and 27 nM, respectively (Table 1). The inhibition of these cellular kinase activities was well correlated with the effects on cellular viability and cell proliferation, and the results are comparable with those obtained with imatinib (Table 1 and Supplemental Data).

Crystallographic structural analysis of AMN107-Abl complexes

Structural analysis of the binding of AMN107 and imatinib to Abl can explain the differential sensitivity of Abl point mutations to these two compounds. The binding modes of AMN107 to the tyrosine kinase domains of both wild-type Abl and the Abl^{M351T} mutant were elucidated from the crystal structures of the complexes (Figure 3). Additional details of the structure of Abl in complex with AMN107 are described elsewhere (P.W.M., unpublished data). Here we report two structures of AMN107 in complex with Abl^{M351T} solved in two different space groups, such that common differences between the structures and the wild-type Abl-AMN107 complex probably result from the mutation and not from artifacts such as crystal contacts. In all of the structures, AMN107 was found to bind to the inactive conformation of Abl as observed for imatinib (Nagar et al., 2003). In the Abl-AMN107 structure, the helix containing Met351 (residues 338–358) is locked into position by the methionine side-chain hooking into a cavity adjacent to Leu364. However,

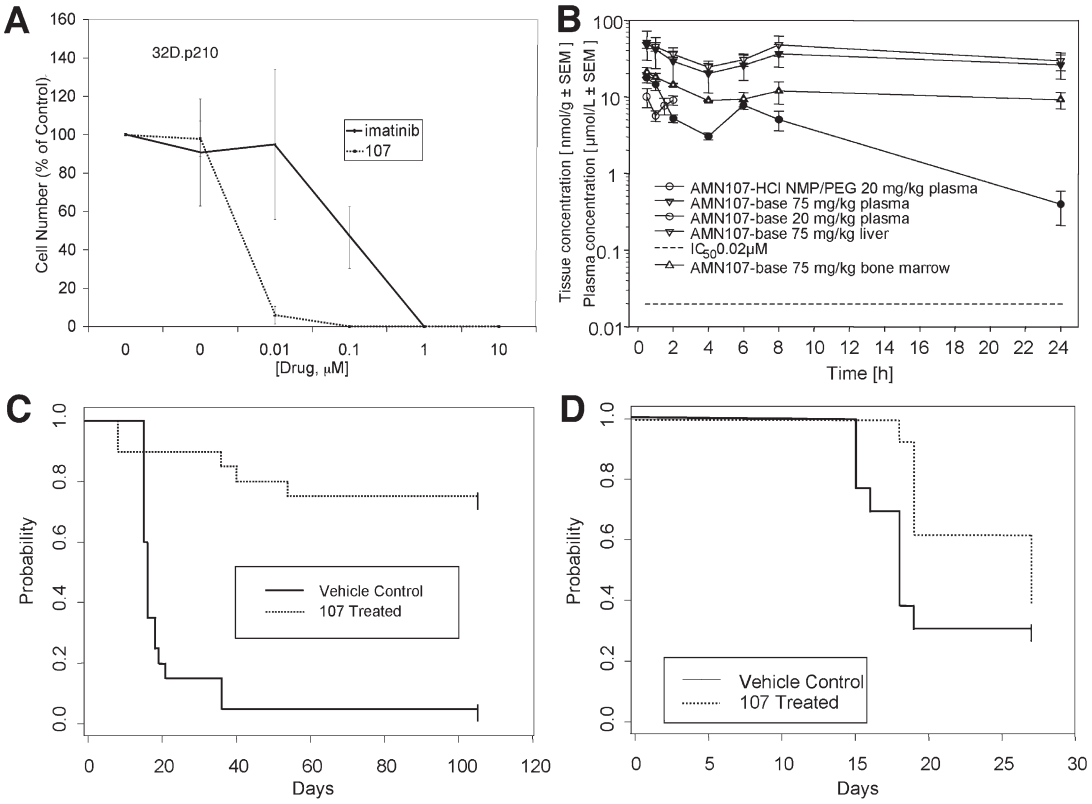

Figure 4. In vivo investigation of AMN107 against 32D.p210 and 32D-E255V cells

A: 32D.p210 cells following 3 days of treatment with increasing concentrations of imatinib or AMN107. Bars are SEM, n = 4.

B: Mean plasma concentrations of AMN107-base following a single oral dose of either 20 mg/kg or 75 mg/kg to naïve mice. Different groups (n = 4) of female OF1 mice received a single oral dose of 20 mg/kg in the respective formulation (based on the free base). The AMN107-base was formulated in 10% N-methyl pyrrolidone/90% PEG200 (v/v). At the allotted times, mice were sacrificed, blood and tissue removed, and the concentration of compound determined by reversed-phase HPLC/MS-MS analysis. Bars are SEM, n = 4. The limit of quantitation (LOQ) was set to 5 ng/ml. Antiproliferative IC_{50} against Ba/F3 Bcr-Abl p210 cells (0.022 μM) is inserted.

C: Kaplan-Meier plot of survival for 32D.p210-injected Balb/c mice treated with either vehicle or AMN107.

D: Kaplan-Meier plot of survival for 32D-E255V-injected Balb/c mice treated with either vehicle or AMN107.

within Abl^{M351T}, this hook is absent, and the whole helix can translate up to 1 Å along its axis. This translation slightly shifts the residues in the loop preceding helix E, which are involved in contacting the SH2 domain in the assembled inactive state (Nagar et al., 2003), and also form part of the myristate binding site.

AMN107 prolongs survival of mice with Bcr-Abl+ leukemias

The pharmacokinetic properties of AMN107 were evaluated following single administration of a solution of either 20 or 75 mg/kg in 10% NMP/90% PEG300 by gavage to naïve female Balb/c mice. Sample analysis was based on an HPLC-MS method with LOQ 0.01 μM, and pharmacokinetic parameters were calculated from the concentration versus time profiles. AMN107 was orally bioavailable and well absorbed, with mean plasma levels of 5.6, 5.4, and 0.4 μM, or 29, 30, and 25 μM, at 2, 8, and 24 hr following administration of either 20 mg/kg (AUC_{0-24h} 82 hr/μmol/l) or 75 mg/kg (AUC_{0-24h} 641 hr/μmol/l), respectively (details are presented in Figure 4B and Table 2).

To directly assess the in vivo antitumor efficacy of AMN107, we developed mouse models of CML in which tumor burden was quantified by noninvasive imaging of the luminescent tumor cells. Murine 32D.p210 cells were engineered to stably express firefly luciferase and evaluated for their responsiveness to imatinib and AMN107 in vitro: AMN107 inhibited the proliferation of 32D.p210 cells in vitro with a mean IC_{50} of 9 nM (imatinib IC_{50} 300 nM; Table 1 and Figure 4A).

Sublethally irradiated NOD-SCID mice were then inoculated with these cells and noninvasive imaging was used to serially assess tumor burden. Mice with established leukemia were divided into cohorts with equivalent tumor burden, and oral administration was initiated with AMN107 or vehicle (Figure 5). Mice with 32D.p210-Luc+ leukemia treated with AMN107 (100 mg/kg/day) showed a profound and rapid reduction in tumor burden (Figure 5). After 4 doses, there was a one-log reduction in overall leukemia burden in AMN107-treated mice, in comparison to a 1.5 log increase in tumor burden in vehicle-treated mice. The results suggested that AMN107 could reduce the accumulation of leukemic cells in marrow, spleen, lymph node areas, and liver.

To determine if this ability to suppress leukemic cell growth

Table 2. Pharmacokinetic parameters of AMN107/AA-salt following single oral administration of either 20 mg/kg or 75 mg/kg to naïve mice

PK parameters	20 mg/kg plasma	75 mg/kg plasma	75 mg/kg bone marrow	75 mg/kg liver
C_{max} (µmol/l; nmol/g)	17.92 ± 2.71	47.90 ± 14.34	21.05 ± 3.14	51.11 ± 2.85
C_{last} (µmol/l; nmol/g)	0.39 ± 0.18	29.69 ± 7.80	9.20 ± 2.22	26.18 ± 10.57
t_{max} (h)	0.5	0.5	0.5	0.5
t_{last} (h)	24	24	24	24
AUC_{0-24h} (h·µmol/l)	81.8	879	261	722
$AUC_{0-24h, dose}$ ([h·µmol/l] [mg/kg])	4.0	11.7	3.48	9.6

Area under the plasma concentration versus time curve (AUC) was calculated from the mean concentrations by linear/log trapezoidal rule using noncompartmental analysis (WinNonlin, Pharsight). The pharmacokinetic parameters Cmax, Clast, tmax, and tlast were determined by inspection of the data.

would prolong survival, AMN107 was administered to a larger cohort of Balb/c mice at an oral dose of 75 mg/kg/day over a 16-day period, commencing three days after injection of 32D.p210 cells. Vehicle-treated animals (19/20) developed a lethal disease (median survival 16 days, range 15–36 days), characterized by splenomegaly (Figure 4C). One control mouse failed to develop signs of leukemia, but was included in the survival analysis. Treatment with AMN107 resulted in the survival of 15/20 animals over 105 days of observation.

Five of the AMN107-treated mice either died or were sacrificed; median survival was not reached. All remaining mice were sacrificed at the planned end of the study (day 105), and were censored in the survival analysis. Body weights and spleen weights were available for 17/20 AMN107-treated mice, and were found to be within the normal range (median body weight 21.9 g, median spleen weight 0.085 g; spleen as a % of body weight: 0.4%). In comparison, vehicle-treated mice had a median body weight of 16.6 g and a median spleen weight of 0.51 g (spleen as % of body weight: 3.2%). Using the Wilcoxon rank sum test, these parameters differed significantly between the vehicle control and the AMN107-treated mice, with p values < 0.0001 for body weight, = 0.0001 for spleen weight, and <0.0001 for spleen as a percentage of body weight. p values were two-sided, and were obtained from the normal approximation to the Wilcoxon. Treatment with AMN107 was associated with a significant prolongation of survival, $p < 0.00001$. The log rank test was used to assess differences in survival.

The effects of AMN107 were also evaluated in a bone marrow transplant model. Bone marrow cells from normal Balb-c mice were transduced with Bcr-Abl and transferred to sublethally irradiated hosts. Such mice develop a reproducible myeloproliferative disease similar to human CML. Groups of mice (n = 12) were treated with vehicle (control), imatinib (125 mg/kg/day in two divided doses), or AMN107 (75 mg/kg daily) by oral gavage, which was started on day 8 following transplant. Mice were sacrificed when moribund as assessed by consistent standard criteria.

The animals in the control group developed splenomegaly and marked leukocytosis as observed previously (Mohi et al., 2004), and all were sacrificed by day 18 posttransplantation (Figure 6). There was a significantly prolonged survival in mice treated with either imatinib or AMN107, all of which were alive at the study end point 20 days after transplantation ($p < 0.001$, Figure 6A). Disease burden, as evidenced by spleen weights at the time of sacrifice, was compared for mice treated with imatinib and AMN107. There was a significant reduction in tumor bulk in mice treated with AMN107 ($p < 0.001$, Figure 6D). In contrast, imatinib failed to control spleen weights despite prolonged survival at 20 days.

AMN107 prolongs survival of mice with leukemia due to imatinib-resistant mutants of Bcr-Abl

The results shown in Figures 4–6 demonstrate that AMN107 is effective in prolonging survival in mice with Bcr-Abl+ leukemias. To determine if AMN107 would also prolong survival in mice with imatinib-resistant Bcr-Abl+ leukemias, we replaced native Bcr-Abl with E255V Bcr-Abl in both the 32D.p210 cell line and BMT models. The E255V mutant is known to be resistant to imatinib (Hofmann et al., 2002; Shah et al., 2002; von Bubnoff et al., 2002; Table 1 and Figure 2). An oral dose of 75 mg/kg/day AMN107 administered over a 16-day period, commencing three days after injection of parental 32D.p210-E255V

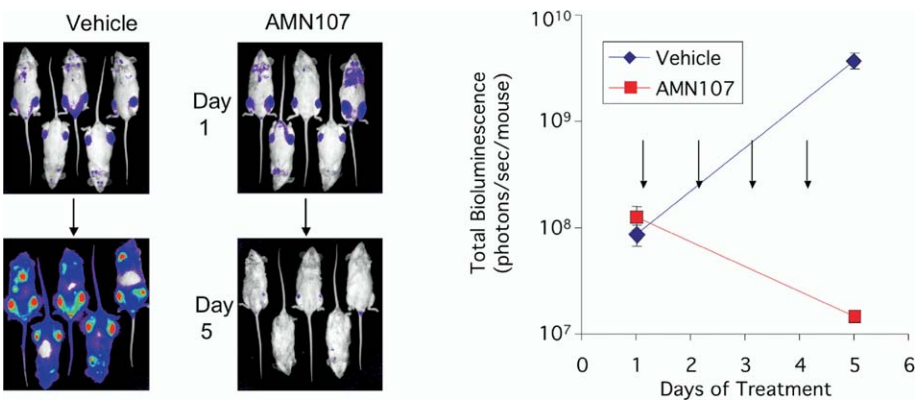

Figure 5. Efficacy of AMN107 against 32D.p210- and 32D-E255V-Luc+ cells in vivo

Left panel: Bioluminescence of vehicle- or AMN107-treated mice. Right panel: Quantitation of AMN107 effects against 32D.p210-Luc+ cells in vivo. Bars are SEM, n = 5.

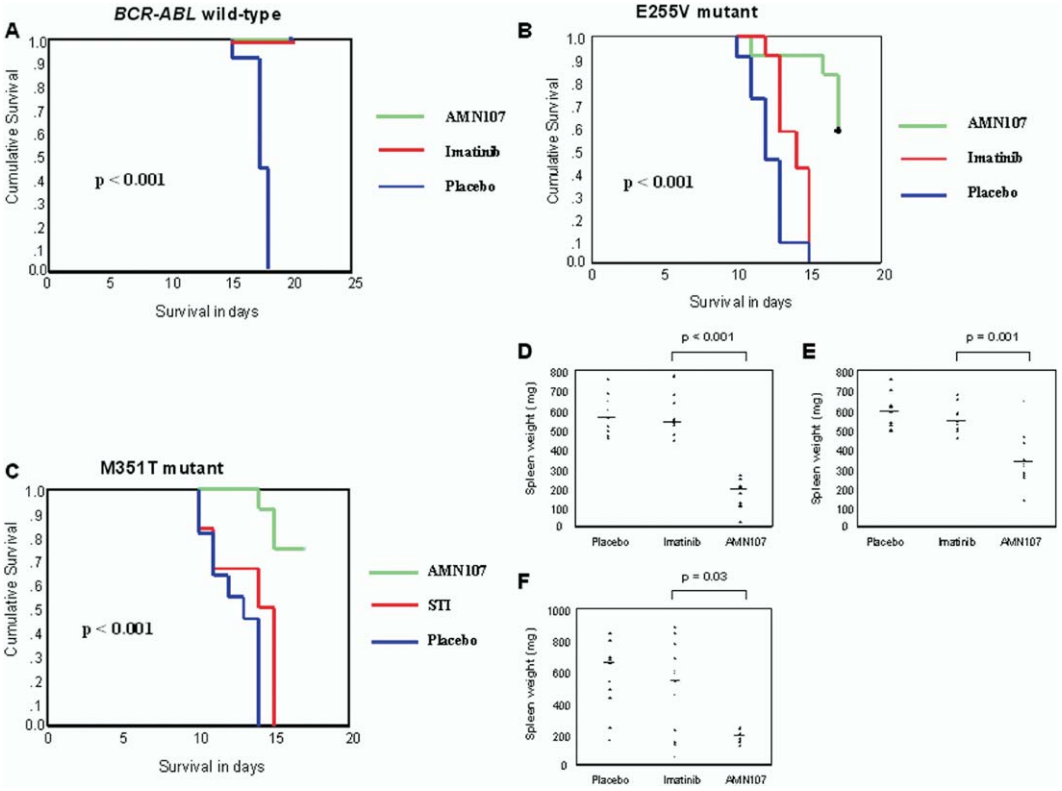

Figure 6. AMN107 treatment prolongs survival and decreases tumor burden in an imatinib-resistant Bcr-Abl mutant BMT model

A–C: Kaplan-Meier plots demonstrating survival for mice transplanted with marrow transduced with wild-type Bcr-Abl (**A**), the imatinib-resistant Bcr-Abl mutant E255V (**B**), and the imatinib-resistant Bcr-Abl mutant M351T (**C**). A significant difference in survival was demonstrated between mice treated with AMN107 and imatinib (log-rank test, $p < 0.001$ for the E255V and M351T mutants).

D–F: Scatter diagrams demonstrating spleen weights for mice treated with either placebo, imatinib, or AMN107 for mice transplanted with marrow transduced with wild-type Bcr-Abl (**D**), the imatinib-resistant Bcr-Abl mutant E255V (**E**), or the imatinib-resistant Bcr-Abl mutant M351T (**F**). Horizontal bars represent median values. Comparisons between values for mice treated with imatinib and AMN107 demonstrate a significant reduction in spleen weights for AMN107-treated animals (p values shown).

cells, resulted in a delayed onset of leukemia in drug-treated mice versus vehicle-treated controls (Figure 4D). The Wilcoxin p value for a difference in time of onset of tumor development was 0.04.

A similar trial was performed for mice transplanted with bone marrow transduced with the imatinib-resistant E255V mutant of *BCR-ABL*, and treated with vehicle, imatinib, or AMN107. Animals in the vehicle-treated control group (12 mice) again developed myeloproliferative disease, as did the mice treated with imatinib, and all were sacrificed by day 15 posttransplantation (Figure 6B). In contrast, treatment with AMN107 significantly prolonged survival in mice transplanted with the E255V mutant, with 7/12 mice still alive at the study endpoint, 17 days posttransplant ($p < 0.001$, Figure 6B). Tumor burden was again compared between mice treated with imatinib or AMN107, and a significant reduction in spleen weight was demonstrated for those animals treated with AMN107 (Figure 6E). Similar results were obtained when the M351T mutant was tested in mice treated with imatinib or AMN107, with significantly prolonged survival in AMN107-treated mice ($p < 0.001$, Figure 6C), and a significant reduction in spleen weight in mice treated with AMN107 (Figure 6F). Liver weights and white cell counts (wcc) were also used as a determinant of tumor burden in mice transplanted with native, E255V, and M351T-Bcr-Abl, and, similar to spleen, a significant reduction was observed in AMN107-treated mice (Supplemental Data). Taken together, these results show that AMN107 can prolong survival of mice with two different imatinib-resistant mutants of Bcr-Abl. However, in both murine models, survival of AMN107-treated mice with native Bcr-Abl appeared to be superior to that of mice with either E255V or M351T mutants, consistent with the fact that these mutants are 27- and 2-fold less sensitive to AMN107 than is native Bcr-Abl (Table 1).

Discussion

Imatinib, an orally administered drug that inhibits the tyrosine kinase activity of Bcr-Abl and of the c-Kit and PDGF receptors, has proven to be an effective treatment for CML- and c-Kit-positive gastrointestinal stromal tumors (GISTs) (Buchdunger et al., 1996; Druker et al., 1996; Carroll et al., 1996; Buchdunger et al., 2000; Demetri et al., 2002). In chronic phase CML, imatinib induces complete hematologic remissions in almost all patients, and in a substantial number produces cytogenetic responses (O'Brien et al., 2003). However, resistance to imatinib occurs in a small number of chronic phase patients, with some

patients relapsing after months or years of treatment. Chronic phase CML patients who achieve a 1000-fold reduction in *BCR-ABL* transcript levels have a negligible risk of disease progression over the subsequent 12 months; this level of cytogenetic response has been achieved in 39% of patients receiving a standard dose regimen of imatinib (O'Brien et al., 2003). In contrast, patients diagnosed with Ph+ ALL, as well as many patients with more advanced stage CML (accelerated phase and blast crisis), fail to achieve a complete cytogenetic response and frequently develop resistance to therapy and relapse (Sawyers et al., 2002; Ottmann et al., 2002).

Resistance to imatinib often results from the emergence of clones expressing mutant forms of Bcr-Abl that exhibit a decreased sensitivity toward inhibition by imatinib. These include G250E, Y253H, E255K(V), T315I, F317L, and M351T (Branford et al., 1999; Gorre et al., 2001; Barthe et al., 2001; Hochhaus et al., 2001; Barthe et al., 2002; Ricci et al., 2002), and more than 30 such mutants have now been isolated from patients (Hochhaus and La Rosee, 2004). Crystallographic studies revealed that imatinib binds to Bcr-Abl by filling a pocket created in the ATP binding site by the DFG motif of the activation loop being displaced from the position that it occupies in the catalytically active conformation of the enzyme (Schindler et al., 2000; Nagar et al., 2003). Point mutations of Bcr-Abl have been characterized as either those that destabilize this inactive protein conformation, or those that sterically impede direct contact between the protein and imatinib (Shah et al., 2002; Corbin et al., 2003; Cowan-Jacob et al., 2004). In general, point mutations affecting residues in close contact with imatinib confer a greater degree of resistance than those affecting the stability of the protein conformation.

A number of strategies to prevent the emergence of resistant clones have been proposed, including combination of imatinib with other agents (Krystal, 2001). Additive/synergistic effects have been achieved when imatinib was combined with standard chemotherapeutic agents such as interferon α, daunorubicin, cytosine arabinoside, and homoharringtonine (Thiesing et al., 2000; Tipping et al., 2002). Agents that disrupt signaling pathways associated with Bcr-Abl or that lead to accelerated catabolism of the Bcr-Abl protein have also been tested for synergy with imatinib (Sun et al., 2001; Gorre et al., 2002; Hoover et al., 2002; Nimmanapalli et al., 2002; Klejman et al., 2002; Nakajima et al., 2003; Warmuth et al., 2003). These alternative strategies are being clinically evaluated alone and in combination with imatinib.

There has also been increasing interest in identifying new Bcr-Abl inhibitors with greater potency than imatinib, or that retain the ability to inhibit imatinib-resistant point mutants to Bcr-Abl (Mow et al., 2002; La Rosee et al., 2002; Shah et al., 2004; O'Hare et al., 2004). Dual Abl and Src kinase inhibitors have the potential attraction that Src may be involved in signaling by Bcr-Abl (Danhauser-Riedl et al., 1996). However, it does not appear that Lyn, hck, or Fgr are important for myeloid disease in mice (Hu et al., 2004), and preliminary studies with agents such as BMS354825 suggest that inhibition of Src kinases in the setting of the highly drug-resistant T315I mutant of Bcr-Abl results in no inhibition at all. The added value of such agents, and potential for added toxicity, will need to be studied in clinical trials.

AMN107 is a new and highly potent inhibitor of Abl that has certain advantages over imatinib. First, AMN107 is 10- to 50-fold more potent as an inhibitor of Bcr-Abl than imatinib, as assessed by its ability to block proliferation of Bcr-Abl dependent cell lines derived from CML patients (K562, Ku-812F) and cell lines (32D or Ba/F3) transfected to express the Bcr-Abl protein. Similarly, AMN107 is 10- to 20-fold more active than imatinib in reducing Bcr-Abl autophosphorylation (IC_{50} values ranging from 20–60 nM). Proliferation of the parental 32D and Ba/F3 cell lines was unaffected at 100-fold greater concentrations, indicating a lack of general toxicity. Similarly, normal myeloid progenitor cells are not inhibited at concentrations of AMN107 <100 nM, and mice show no evidence of hematopoietic toxicity after exposure to high concentrations of drug for 14 days.

AMN107 also inhibited the tyrosine kinase activity of the PDGF and c-Kit receptors, displaying similar efficacy to imatinib, and therefore possessing greater selectivity toward Bcr-Abl. AMN107 showed no activity against a wide panel of other protein kinases at concentrations below 3 μM, including c-Src.

A key feature of AMN107 is the ability to inhibit some Bcr-Abl point mutants resistant to imatinib. The majority of the 15 mutants tested were sensitive to AMN107 to a variable degree, with IC_{50} values ranging from <10 nM to approximately 1000 nM (when assessed in proliferation assays in vitro), with 10 mutants <100 nM (Table 1). Mutants G250E, Q252H, Y253H, E255K/V, T315I, and M351T are the most common mutants in patients with imatinib resistance (>5% incidence each), while the others tested are detected in 1% to 5% of patients (Hochhaus and La Rosee, 2004). Overall, L248R, Y253H, E255K/V, and L248R were the least sensitive to AMN107, with IC_{50} values 100–1000 nM, while T315I was resistant at an IC_{50} value of >10,000 nM. Since plasma levels of AMN107 in excess of 10,000 nM can be readily achieved in mice, these results suggest that many imatinib-resistant Bcr-Abl mutants might be effectively targeted by AMN107.

In an effort to explain the differences between imatinib and AMN107 as inhibitors of Abl, crystallographic structural analysis of an Abl-AMN107 complex was performed. Like imatinib, AMN107 binds to the inactive conformation of Abl kinase (Cowan-Jacob et al., 2004). From analysis of crystal structures, the greater affinity of AMN107 compared to imatinib results from a better topological fit of AMN107 to the protein, contrasting with the need to desolvate/deprotonate the highly basic *N*-methylpiperazine and the slightly larger constraints on the binding surface for this group in imatinib. The binding affinity contributed by the pyridinyl and pyrimidinyl groups is therefore relatively large for imatinib, and small compared to the total energy for AMN107, where the trifluoromethyl/imidazole substituted phenyl group (Figure 1A) contributes greatly to the potency. Hence, mutations such as F317L from the hinge region and E255K/V in the P loop, which contact the pyridinyl and pyrimidinyl groups, have less effect on the overall affinity of AMN107 than imatinib. The crystal structure of Abl^{M351T} shows that residues of the C-terminal lobe lining the imatinib binding site are only marginally affected by the M351T mutation, and could explain the small reduction in affinity to Abl^{M351T} compared to wt-Abl, although energetic differences between the two states might be of greater importance. If imatinib must induce Abl to adopt a specific conformation for binding, then the affinity will be greater if that conformational state is of lower energy. The M351T mutation facilitates other positions of helix E, increasing the entropy and thus increasing the energy re-

quired to adopt the imatinib binding mode. This mutation has little effect on AMN107 affinity, since there is less stringent induced-fit binding. In contrast to imatinib, which makes directional H bonds to Ile360 and His361, the imidazole moiety has less critical interactions with the C-terminal lobe. Similar energetic effects would be expected for other mutants, e.g. M244V and F486S, which are distant from the imatinib binding site and cause mild resistance to imatinib. The T315I mutant remains insensitive to binding of AMN107 due to the loss of a hydrogen bond and introduction of a steric clash, as in the case of imatinib (Schindler et al., 2000). A different inhibitor scaffold would be required to overcome resistance to this mutant. The reduced sensitivity of the G250E mutant toward AMN107 is probably because the glutamate stabilizes the active conformation of Abl. This is in contrast to other mutations in this region, such as Y253F/H and E255K/V, which destabilize the inactive conformation of the P loop (Cowan-Jacob et al., 2004).

Having demonstrated the potent in vitro efficacy of AMN107, we evaluated the compound against Bcr-Abl-induced leukemia in animal models. AMN107 was well absorbed and displayed good bioavailability in mice; oral administration of 20 mg/kg of AMN107 yielded a mean plasma level in the range of 6.0–12.1 μM after 2 hr, which is >100-fold greater than the concentrations required to inhibit either Bcr-Abl autophosphorylation or hematopoietic cell proliferation in vitro. Following a single 75 mg/kg dose, high plasma and bone marrow concentrations were maintained out to 24 hr, and the compound was well tolerated at oral doses up to 150 mg/kg/day.

The potential of AMN107 for in vivo activity was tested in a short-term model where nude mice were injected with 32Dp210Bcr/Abl cells additionally expressing the luciferase gene. Serial imaging indicated that compared to vehicle, AMN107 dramatically reduced the accumulation of leukemic cells in the bone marrow, spleen, liver, and lymph node areas, indicating effective distribution into multiple tissues in vivo. To determine whether AMN107 could also extend the survival of mice injected with 32Dp210Bcr-Abl cells, Balb/c mice were treated with an oral dose of 75 mg/kg q.d. over a 16-day period, commencing three days after the injection of 32D.p210 Bcr-Abl cells, or vehicle control. Treatment with AMN107 resulted in the survival of 15/20 animals over the 105 days of planned observation, whereas 19/20 vehicle-treated mice had progressive disease. Spleen weights of the animals receiving AMN107 were within the normal range at the end of the experiment. Taken together, these two studies with 32Dp210Bcr-Abl cell lines indicate the potential of AMN107 to rapidly and profoundly suppress disease development.

To determine if the therapeutic effects of AMN107 on Bcr-Abl+ cell lines would extend to Bcr-Abl+ primary hematopoietic cells, mice were transplanted with marrow infected with a Bcr-Abl retrovirus, followed 8 days later by treatment with AMN107, imatinib, or vehicle control. In this model, mice develop a highly reproducible CML-like myeloproliferative syndrome characterized by granulocytosis and splenomegaly. Treatment with AMN107 reduced morbidity and, at the end of the study, yielded spleen weights within the normal range, as observed for the long-term survival experiments.

As noted above, the availability of agents that could be used to treat imatinib-resistant clones of Bcr-Abl+ leukemias would have significant therapeutic value. This possibility was assessed using a highly imatinib-resistant mutant, E255V Bcr-Abl, both in mice injected with 32D.p210-E255V cells and in mice receiving bone marrow transplants after infection with the Bcr-Abl mutant, E255V. In both of these models, AMN107, but not imatinib, increased survival and decreased disease volume. These results were extended by testing a second imatinib-resistant mutant, M351T. AMN107 significantly prolonged survival compared to imatinib ($p < 0.001$, Figure 6E), and also resulted in a significant reduction in spleen weight and other measures of disease burden (Figure 6F).

Overall, the data presented here suggest that AMN107 is highly cytotoxic to both cell lines and primary hematopoietic cells expressing Bcr-Abl, and that it could have certain advantages over imatinib in terms of higher potency and the ability to inhibit some imatinib-resistant mutants. However, since the IC_{50} value of AMN107 for some imatinib-resistant mutants is higher than for wild-type Bcr-Abl, it may be necessary to achieve substantially higher plasma concentrations of AMN107 in such patients to achieve responses.

If human clinical trials validate the effectiveness of AMN107 demonstrated in the preclinical studies reported here, it may be possible to either use AMN107 in selected patients with imatinib resistance, or to use both agents together, simultaneously or sequentially. Highly potent inhibitors of Bcr-Abl should reduce the number of residual Bcr-Abl+ cells capable of undergoing mutation. Consequently, monotherapy with highly potent Abl inhibitors, or combinations of Abl inhibitors with different mechanisms of action, might prevent or delay the emergence of some types of drug-resistant mutants of Bcr-Abl. In support of simultaneous administration, AMN107 was shown to be synergistic when combined with imatinib against cells expressing p210Bcr-Abl or p190Bcr-Abl, despite the fact that both inhibitors bind to the same site.

While we anticipate that new Bcr-Abl point mutations could eventually emerge to confer resistance to AMN107, it may be possible to cycle or combine agents to suppress or delay the emergence of resistant clones. Thus, the availability of novel, high-potency, Abl tyrosine kinase inhibitors will usher in a new generation of clinical studies that will hopefully result in additional major advances in the therapy of CML and Ph+ ALL.

Experimental procedures

Systemic 32D Bcr-Abl leukemia model

32D.p210 and 32D-E255V cells free of *Mycoplasma* and viral contamination were washed once with Hank's Balanced Salt Solution (HBSS; Mediatech, Inc.,VA), and resuspended in HBSS prior to administration to mice. Solutions of AMN107 were prepared just prior to administration, by dissolving 75 mg in 1.0 ml of NMP to give a clear solution and diluting with 9.0 ml PEG300. Female BALB/c mice (weighing 15–18 g and 6–7 weeks of age at delivery; Taconic, NY) were administered suspensions containing 32D.p210 or 32D-E255V cells by tail vein injection (1×10^5 32D.p210 cells/mouse; 7×10^5 32D-E255V cells/mouse; day 0). 32D.p210-injected mice were treated via gavage with either vehicle (10% NMP-90% PEG300) or AMN107 (75 mg/kg/day) on days 3, 4, 7, 8, 9, 10, 11, 15, 16, 17, and 18 (eleven doses total), and monitored for signs of leukemia. 32D-E255V-injected mice were treated via gavage with either vehicle or AMN107 (100 mg/kg/day) once daily for 21 days. Mice were sacrificed if they became morbid, according to institute protocols. At the planned end of each study, any remaining mice were sacrificed, body and spleen weights were recorded, and tissues preserved in 10% formalin for histopathological analysis.

Survival was measured as time from cell injection to death or sacrifice. All starting animals were included in the statistical analysis. Survival analysis was performed using the method of Kaplan and Meier with statistical significance assessed using the log rank test.

Bioluminescent Bcr-Abl model of CML

Cells were transduced with a retrovirus encoding firefly luciferase (MSCV-Luc), and selected with puromycin at 2 μg/ml to produce 32D.p210-Luc+ and 32D-E255V-Luc+ cell lines. Female NOD-SCID mice (8–10 weeks of age; Jackson Laboratory) were sublethally irradiated with a single fraction of 300 rads, and 3–6 hr later, a total of 1×10^6 cells were administered by tail vein injection. Mice were imaged and total body luminescence quantified as previously described (Armstrong et al., 2003). Baseline imaging 5–7 days after tumor cell inoculation was used to establish treatment cohorts with matched tumor burden. Cohorts of mice were treated with oral administration of vehicle (formulated as above), 75 mg/kg imatinib (twice daily), or 100 mg/kg/day AMN107 (formulated as above). Repeat imaging was performed every 3–4 days.

Bone marrow transplant Bcr-Abl model of CML

The murine BMT assays and drug treatment were performed as described previously (Liu et al., 2000; Cools et al., 2003; Kelly et al., 2002). In brief, 1×10^6 bone marrow cells transduced with distinct retroviral constructs (either native p210-BCR-ABL or BCR-ABL E255V mutant both in MSCV-IRES-GFP) were injected into the lateral tail veins of lethally irradiated (450cGy X2) syngeneic Balb/c recipient mice. After 8 days, mice were administered either vehicle (10% NMP-90% PEG300), 75 mg/kg/day AMN107 (formulated in 10% NMP-90% PEG300), or 125 mg/kg/day imatinib (two divided doses formulated in 0.05% methylcellulose) via oral gavage. Diseased animals, identified by splenomegaly or moribund appearance, were sacrificed. Spleen and liver weights were recorded and histopathological analyses were performed for each animal; single-cell suspensions of bone marrow, spleen, and peripheral blood were analyzed by flow cytometry as described previously (Schwaller et al., 1998). Survival analysis was performed using the method of Kaplan and Meier with statistical significance assessed using the log rank test. Tumor burden as assessed by white cell counts (WCC) and spleen and liver weights were compared by the Mann-Whitney U test for each treatment category.

Supplemental data

Information on cell lines and cell culture, chemical compounds and biologic reagents, antibodies, cell proliferation studies, apoptosis assays, immunoprecipitation and immunoblotting, effects of imatinib and AMN107 on phosphorylation status of target kinases in cells, determination of AMN107 binding sites in Abl (including preparation of the c-Abl^{M351T}-AMN107 complex, crystal structure determination of the c-Abl^{M351T}-AMN107 complex, and structure determination and refinement), and synergy studies can be found in the Supplemental Data at http://www.cancercell.org/cgi/content/full/7/2/129/DC1/.

Acknowledgment

J.D.G. and D.G.G. are supported by NIH grant CA66996, and a Specialized Center of Research Award from the Leukemia and Lymphoma Society. J.D.G. is also supported by NIH grants CA36167 and DK50654. G.Q.D. is supported by grants from the National Cancer Institute (CA86991), the NIH Director's Pioneer Award (DP1-OD000256), and the Burroughs Wellcome Fund. P.W.M., W.B., J.B., S.W.C.-J., D.F., G.F., and J.M. are employees of Novartis Pharma AG, Basel, Switzerland. J.D.G has a financial interest with Novartis Pharma AG. B.H. is a senior clinical fellow of the LRF (UK).

Received: August 9, 2004
Revised: October 27, 2004
Accepted: January 18, 2005
Published: February 14, 2005

References

Armstrong, S.A., Kung, A.L., Mabon, M.E., Silverman, L.B., Stam, R.W., Den Boer, M.L., Pieters, R., Kersey, J.H., Sallan, S.E., Fletcher, J.A., et al. (2003). Validation of a therapeutic target identified by gene expression based classification. Cancer Cell *3*, 173–183.

Azam, M., Latek, R.R., and Daley, G.Q. (2003). Mechanisms of autoinhibition and STI-571/imatinib resistance revealed by mutagenesis of BCR-ABL. Cell *112*, 831–843.

Barthe, C., Cony-Makhoul, P., Melo, J.V., and Mahon, J.R. (2001). Roots of clinical resistance to STI-571 cancer therapy. Science *293*, 2163.

Barthe, C., Gharbi, M.J., Lagarde, V., Chollet, C., Cony-Makhoul, P., Reiffers, J., Goldman, J.M., Melo, J.V., and Mahon, F.X. (2002). Mutation in the ATP-binding site of BCR-ABL in a patient with chronic myeloid leukaemia with increasing resistance to STI571. Br. J. Haematol. *119*, 109–111.

Bedi, A., Zehnbauer, B.A., Barber, J.P., Sharkis, S.J., and Jones, R.J. (1994). Inhibition of apoptosis by BCR-ABL in chronic myeloid leukemia. Blood *83*, 2038–2044.

Branford, S., Hughes, T.P., and Rudzki, Z. (1999). Monitoring chronic myeloid leukaemia therapy by real-time quantitative PCR in blood is a reliable alternative to bone marrow cytogenetics. Br. J. Haematol. *107*, 587–599.

Branford, S., Rudzki, Z., Walsh, S., Grigg, A., Arthur, C., Taylor, K., Herrmann, R., Lynch, K.P., and Hughes, T.P. (2002). High frequency of point mutations clustered within the adenosine triphosphate-binding region of BCR/ABL in patients with chronic myeloid leukemia or Ph-positive acute lymphoblastic leukemia who develop imatinib (STI571) resistance. Blood *99*, 3472–3475.

Buchdunger, E., Zimmermann, J., Mett, H., Meyer, T., Muller, M., Druker, B.J., and Lydon, N.B. (1996). Inhibition of the Abl protein-tyrosine kinase in vitro and in vivo by a 2-phenylaminopyrimidine derivative. Cancer Res. *56*, 100–104.

Buchdunger, E., Cioffi, C.L., Law, N., Stover, D., Ohno-Jones, S., Druker, B.J., and Lydon, N.B. (2000). Abl protein-tyrosine kinase inhibitor STI571 inhibits in vitro signal transduction mediated by c-kit and platelet-derived growth factor receptors. J. Pharmacol. Exp. Ther. *295*, 139–145.

Buchdunger, E., Matter, A., and Druker, B.J. (2001). Bcr-Abl inhibition as a modality of CML therapeutics. Biochim. Biophys. Acta *1551*, M11–M18.

Campbell, L.J., Patsouris, C., Rayeroux, K.C., Somana, K., Januszewicz, E.H., and Szer, J. (2002). BCR-ABL amplification in chronic myelocytic leukemia blast crisis following imatinib mesylate administration. Cancer Genet. Cytogenet. *139*, 30–33.

Carroll, M., Tomasson, M.H., Barker, G.F., Golub, T.R., and Gilliland, D.G. (1996). The Tel platelet-derived growth factor receptor (PDGF-beta-R) fusion in chronic myelomonocytic leukemia is a transforming protein that self-associates and activates PDGF-beta-R kinase-dependent signaling pathways. Proc. Natl. Acad. Sci. USA *93*, 14845–14850.

Cools, J., Stover, E.H., Boulton, C.L., Gotlib, J., Legare, R.D., Amaral, S.M., Curley, D.P., Duclos, N., Rowan, R., Kutok, J.L., et al. (2003). PKC412 overcomes resistance to imatinib in a murine model of FIP1L1-PDGFRalpha-induced myeloproliferative disease. Cancer Cell *3*, 459–469.

Corbin, A.S., La Rosee, P., Stoffregen, E.P., Druker, B.J., and Deininger, M.W. (2003). Several Bcr-Abl kinase domain mutants associated with imatinib mesylate resistance remain sensitive to imatinib. Blood *101*, 4611–4614.

Cowan-Jacob, S.W., Guez, V., Griffin, J.D., Fabbro, D., Fendrich, G., Furet, P., Liebetanz, J., Mestan, J., and Manley, P.W. (2004). Bcr-Abl kinase mutations and drug resistance to imatinib (STI571) in chronic myelogenous leukemia. Mini Rev. Med. Chem. *4*, 285–299.

Danhauser-Riedl, S., Warmuth, M., Druker, B.J., Emmerich, B., and Hallek, M. (1996). Activation of Src kinases p53/56lyn and p59hck by p210bcr/abl in myeloid cells. Cancer Res. *56*, 3589–3596.

Deininger, M.W.N., Goldman, J.M., and Melo, J.V. (2000). The molecular biology of chronic myeloid leukemia. Blood *96*, 3343–3356.

Demetri, G.D., von Mehren, M., Blanke, C.D., Van den Abbeele, A.D., Eisenberg, B., Roberts, P.J., Heinrich, M.C., Tuveson, D.A., Singer, S., Janicek, M., et al. (2002). Efficacy and safety of imatinib mesylate in advanced gastrointestinal stromal tumors. N. Engl. J. Med. *347*, 472–480.

Druker, B.J., Tamura, S., Buchdunger, E., Ohno, S., Segal, G.M., Fanning, S., Zimmermann, J., and Lydon, N.B. (1996). Effects of a selective inhibitor

of the Abl tyrosine kinase on the growth of Bcr-Abl positive cells. Nat. Med. *2*, 561–566.

Gordon, M.Y., Dowding, C.R., Riley, G.P., Goldman, J.M., and Greaves, M.F. (1987). Altered adhesive interactions with marrow stroma of heamotopoietic progenitor cells in chronic myeloid leukaemia. Nature *328*, 342–344.

Gorre, M.E., Mohammed, M., Ellwood, K., Hsu, N., Paquette, R., Rao, P.N., and Sawyers, C.L. (2001). Clinical resistance to STI-571 cancer therapy caused by BCR-ABL gene mutation or amplification. Science *293*, 876–880.

Gorre, M.E., Ellwood-Yen, K., Chiosis, G., Rosen, N., and Sawyers, C.L. (2002). BCR-ABL point mutants isolated from patients with imatinib mesylate-resistant chronic myeloid leukemia remain sensitive to inhibitors of the BCR-ABL chaperone heat shock protein 90. Blood *100*, 3041–3044.

Hochhaus, A., and La Rosee, P. (2004). Imatinib therapy in chronic myelogenous leukemia: Strategies to avoid and overcome resistance. Leukemia *18*, 1321–1331.

Hochhaus, A., Kreil, S., Corbin, A., La Rosee, P., Lahaye, T., Berger, U., Cross, N.C., Linkesch, W., Druker, B.J., Hehlmann, R., et al. (2001). Roots of clinical resistance to STI-571 cancer therapy. Science *293*, 2163.

Hochhaus, A., Kreil, S., Corbin, A.S., La Rosee, P., Muller, M.C., Lahaye, T., Hanfstein, B., Schoch, C., Cross, N.C., Berger, U., et al. (2002). Molecular and chromosomal mechanisms of resistance to imatinib (STI571) therapy. Leukemia *16*, 2190–2196.

Hofmann, W.K., Jones, L.C., Lemp, N.A., de Vos, S., Gschaidmeier, H., Hoelzer, D., Ottmann, O.G., and Koeffler, H.P. (2002). Ph(+) acute lymphoblastic leukemia resistant to the tyrosine kinase inhibitor STI571 has a unique BCR-ABL gene mutation. Blood *99*, 1860–1862.

Hoover, R.R., Mahon, F.X., Melo, J.V., and Daley, G.Q. (2002). Overcoming STI571 resistance with the farnesyl transferase inhibitor SCH66336. Blood *100*, 1068–1071.

Hu, Y., Liu, Y., Pelletier, S., Buchdunger, E., Warmuth, M., Fabbro, D., Hallek, M., Van Etten, R.A., and Li, S. (2004). Requirement of Src kinases Lyn, Hck and Fgr for BCR-ABL1-induced B-lymphoblastic leukemia but not chronic myeloid leukemia. Nat. Genet. *36*, 453–461.

Kantarjian, H.M., and Talpaz, M. (1988). Definition of the accelerated phase of chronic myelogenous leukemia. J. Clin. Oncol. *6*, 180–182.

Kelly, L.M., Yu, J.C., Boulton, C.L., Apatira, M., Li, J., Sullivan, C.M., Williams, I., Amaral, S.M., Curley, D.P., Duclos, N., et al. (2002). CT53518, a novel selective FLT3 antagonist for the treatment of acute myelogenous leukemia (AML). Cancer Cell *1*, 421–432.

Krystal, G.W. (2001). Mechanisms of resistance to imatinib (STI571) and prospects for combination with conventional chmeotherapeutic agents. Drug Resist. Updat. *4*, 16–21.

Klejman, A., Rushen, L., Morrione, A., Slupianek, A., and Skorski, T. (2002). Phosphatidylinositol-3-kinase inhibitors enhance the anti-leukemia effect of STI571. Oncogene *21*, 5868–5876.

La Rosee, P., Johnson, K., O'Dwyer, M.E., and Druker, B.J. (2002). In vitro studies of the combination of imatinib mesylate (Gleevec) and arsenic trioxide (Trisenox) in chronic myelogenous leukemia. Exp. Hematol. *30*, 729–737.

le Coutre, P., Tassi, E., Varella-Garcia, M., Barni, R., Mologni, L., Cabrita, G., Marchesi, E., Supino, R., and Gambacorti-Passerini, C. (2000). Induction of resistance to the Abelson inhibitor STI571 in human leukemic cells through gene amplification. Blood *95*, 1758–1766.

Liu, Q., Schwaller, J., Kutok, J., Cain, D., Aster, J.C., Williams, I.R., and Gilliland, D.G. (2000). Signal transduction and transforming properties of the TEL-TRKC fusions associated with t(12;15)(p13;q25) in congenital fibrosarcoma and acute myelogenous leukemia. EMBO J. *19*, 1827–1838.

Lugo, T.G., Pendergast, A.M., Muller, A.J., and Witte, O.N. (1990). Tyrosine kinase activitiy and transformation potency of BCR-ABL oncogene products. Science *247*, 1079–1082.

Mahon, F.X., Deininger, M.V., Schultheis, B., Chabrol Reiffers, J., Goldman, J.M., and Melo, J.V. (2000). Selection and characterization of BCR-ABL positive cell lines with differential sensitivity to the tyrosine kinase inhibitor STI571: Diverse mechanisms of resistance. Blood *96*, 1070–1079.

Manley, P.W., Breitenstein, W., Bruggen, J., Cowan-Jacob, S.W., Furet, P., Mestan, J., and Meyer, T. (2004). Urea-derivatives of STI571 as inhibitors of Bcr-Abl and PDGFR kinases. Bioorg. Med. Chem. Lett. *14*, 5793–5797.

Melo, J.V., Myint, H., Galton, D.A., and Goldman, J.M. (1994). P190BCR-ABL chronic myeloid leukaemia: The missing link with chronic myelomonocytic leukaemia? Leukemia *8*, 208–211.

Mohi, M.G., Boulton, C., Gu, T.L., Sternberg, D.W., Neuberg, D., Griffin, J.D., Gilliland, D.G., and Neel, B.G. (2004). Combination of rapamycin and protein tyrosine kinase (PTK) inhibitors for the treatment of leukemias caused by oncogenic PTKs. Proc. Natl. Acad. Sci. USA *101*, 3130–3135.

Morel, F., Bris, M.J., Herry, A., Calvez, G.L., Marion, V., Abgrall, J.F., Berthou, C., and Braekeleer, M.D. (2003). Double minutes containing amplified bcr-abl fusion gene in a case of chronic myeloid leukemia treated by imatinib. Eur. J. Haematol. *70*, 235–239.

Mow, B.M., Chandra, J., Svingen, P.A., Hallgren, C.G., Weisberg, E., Kottke, T.J., Narayanan, V.L., Litzow, M.R., Griffin, J.D., Sausville, E.A., et al. (2002). Effects of the Bcr-Abl kinase inhibitors STI571 and adaphostin (NSC 680410) on chronic myelogenous leukemia cells in vitro. Blood *99*, 664–671.

Nagar, B., Hantschel, O., Young, M., Scheffzek, K., Veach, D., Bornmann, W., Clarkson, B., Superti-Furga, G., and Kuriyan, J. (2003). Structural basis for the autoinhibition of c-Abl tyrosine kinase. Cell *112*, 859–871.

Nakajima, A., Tauchi, T., Sumi, M., Bishop, W.R., and Ohyashiki, K. (2003). Efficacy of SCH66336, farnesyl transferase inhibitor, in conjuction with imatinib against BCR-ABL-positive cells. Mol. Cancer Ther. *2*, 219–224.

Nimmanapalli, R., O'Bryan, E., Huang, M., Bali, P., Burnette, P.K., Loughran, T., Tepperberg, J., Jove, R., and Bhalla, K. (2002). Molecular characterization and sensitivity of STI-571 (imatinib mesylate, Gleevec)-resistant, Bcr-Abl-positive, human acute leukemia cells to SRC kinase inhibitor PD180970 and 17-allylamino-17-demethoxygeldanamycin. Cancer Res. *62*, 5761–5769.

O'Brien, S.G., Guilhot, F., Larson, R.A., Gathmann, I., Baccarani, M., Cervantes, F., Cornelissen, J.J., Fischer, T., Hochhaus, A., Hughes, T., et al. (2003). Imatinib compared with interferon and low-dose cytarabine for newly diagnosed chronic-phase chronic myeloid leukemia. N. Engl. J. Med. *348*, 994–1004.

O'Dwyer, M.E., Mauro, M.J., Kurilik, G., Mori, M., Balleisen, S., Olson, S., Magenis, E., Capdeville, R., and Druker, B.J. (2002). The impact of clonal evolution on response to imatinib mesylate (STI571) in accelerated phase CML. Blood *100*, 1628–1633.

O'Hare, T., Pollock, R., Stoffregan, E.P., Keats, J.A., Abdullah, O.M., Moseson, E.M., Rivera, V.M., Tang, H., Metcalf, C.A., III, Bohacek, R.S., et al. (2004). Inhibition of native and mutant Bcr-Abl by AP23464, a potent ATP-based oncogenic protein kinase inhibitor: Implications for CML. Blood *104*, 2532–2539.

Ottmann, O.G., Druker, B.J., Sawyers, C.L., Goldman, J.M., Reiffers, J., Silver, R.T., Tura, S., Fischer, T., Deininger, M.W., Schiffer, C.A., et al. (2002). A phase 2 study of imatinib in patients with relapsed or refractory Philadelphia chromosome-positive acute lymphoid leukemias. Blood *100*, 1965–1971.

Puil, L., Liu, J., Gish, G., Mbamalu, G., Bowtell, D., Pelicci, P.G., Arlinghaus, R., and Pawson, T. (1994). Bcr-Abl oncoproteins bind directly to activators of the Ras signaling pathway. EMBO J. *13*, 746–773.

Ravandi, F., Cortes, J., Albitar, M., Arlinghaus, R., Qiang Guo, J., Talpaz, M., and Kantarjian, H.M. (1999). Chronic myelogenous leukaemia with p185BCR-ABL expression: Characteristics and clinical significance. Br. J. Haematol. *107*, 581–586.

Ricci, C., Scappini, B., Divoky, V., Gatto, S., Onida, F., Verstovsek, S., Kantarjian, H.M., and Beran, M. (2002). Mutation in the ATP-binding pocket of the ABL kinase domain in an STI571-resistant BCR-ABL-positive cell line. Cancer Res. *62*, 5995–5998.

Roche-Lestienne, C., Soenen-Cornu, V., Grardel-Duflos, N., Lai, J.L., Philippe, N., Facon, T., Fenaux, P., and Preudhomme, C. (2002). Several types of mutations of the Abl gene can be found in chronic myeloid leukemia patients resistant to STI571, and they can pre-exist to the onset of treatment. Blood *100*, 1014–1018.

Sawyers, C.L., Hochhaus, A., Feldman, E., Goldman, J.M., Miller, C.B., Ottmann, O.G., Schiffer, C.A., Talpaz, M., Guilhot, F., and Deininger, M.W. (2002). Imatinib induces hematologic and cytogenetic responses in patients with chronic myelogenous leukemia in myeloid blast crisis: Results of a phase II study. Blood *99*, 3530–3539.

Schindler, T., Bornmann, W., Pellicena, P., Miller, T.W., Clarkson, B., and Kuriyan, J. (2000). Structural mechanism of STI-571 inhibition of abelson tyrosine kinase. Science *289*, 1938–1942.

Schwaller, J., Frantsve, J., Aster, J., Williams, I.R., Tomasson, M.H., Ross, T.S., Peeters, P., Van Rompaey, L., Van Etten, R.A., Ilaria, R., Jr., et al. (1998). Transformation of hematopoietic cell lines to growth-factor independence and induction of a fatal myelo- and lymphoproliferative disease in mice by retrovirally transduced TEL/JAK2 fusion genes. EMBO J. *17*, 5321–5333.

Shah, N.P., Nicoll, J.M., Nagar, B., Gorre, M.E., Paquette, R.L., Kuriyan, J., and Sawyers, C.L. (2002). Multiple BCR-ABL kinase domain mutations confer polyclonal resistance to the tyrosine kinase inhibitor imatinib (STI571) in chronic phase and blast crisis chronic myeloid leukemia. Cancer Cell *2*, 117–125.

Shah, N.P., Tran, C., Lee, F.Y., Chen, P., Norris, D., and Sawyers, C.L. (2004). Overriding imatinib resistance with a novel ABL kinase inhibitor. Science *305*, 399–401.

Sun, X., Layton, J.E., Elefanty, A., and Lieschke, G.J. (2001). Comparison of effects of the tyrosine kinase inhibitors AG957, AG490, and STI571 on BCR-ABL-expressing cells, demonstrating synergy between AG490 and STI571. Blood *97*, 2008–2015.

Thiesing, J.T., Ohno-Jones, S., Kolibaba, K.S., and Druker, B.J. (2000). Efficacy of STI571, an abl tyrosine kinase inhibitor, in conjunction with other antileukemic agents against bcr-abl-positive cells. Blood *96*, 3195–3199.

Tipping, A.J., Mahon, F.X., Zafirides, G., Lagarde, V., Goldman, J.M., and Melo, J.V. (2002). Drug responses of imatinib mesylate-resistant cells: Synergism of imatinib with other chemotherapeutic drugs. Leukemia *16*, 2349–2357.

von Bubnoff, N., Schneller, F., Peschel, C., and Duyster, J. (2002). BCR-ABL gene mutations in relation to clinical resistance of Philadelphia-chromosome-positive leukaemia to STI571: A prospective study. Lancet *359*, 487–491.

Warmuth, M., Simon, N., Mitina, O., Mathes, R., Fabbro, D., Manley, P.W., Buchdunger, E., Forster, K., Moarefi, I., and Hallek, M. (2003). Dual-specific Src and Abl kinase inhibitors, PP1 and CGP76030, inhibit growth and survival of cells expressing imatinib mesylate-resistant Bcr-Abl kinases. Blood *101*, 664–672.

Weisberg, E., and Griffin, J.D. (2000). Mechanism of resistance to the ABL tyrosine kinase inhibitor STI571 in BCR-ABL-transformed hematopoietic cell lines. Blood *95*, 3498–3505.